

## **Physical Modeling of a 3D marine seismic survey**

Joe Wong, Rolf Maier, Eric Gallant, and Don Lawton

### **ABSTRACT**

The U of C Seismic Physical Modeling Facility was used to acquire scaled-down 3D marine seismic data. An array of sixteen receiver piezopins was used to represent a marine hydrophone streamer. Data were collected with two transmitters, one at either end of the receiver array. About 50,000 traces were collected over an area measuring  $X=270\text{mm}$  by  $Y=250\text{mm}$ , with grid spacing of  $\Delta X=\text{mm}$  by  $\Delta Y=\text{mm}$ . The acquisition rate was about 4000 traces per hour. Data were written into SEG Y files, and gathers of seismograms were plotted using PROMAX for visual inspection and evaluation of the data. We found that attenuating the strength of direct arrivals relative to reflection amplitudes before digitization is important for increasing the quality of the reflections. The results of this 3D survey helped us to identify needed improvements in our acquisition procedures.

### **INTRODUCTION**

In an important step in the continuing development and upgrading of the U of C modeling facility (Wong et al., 2009), capability for writing SEG Y files has been added to the acquisition software. Files of seismograms written by the software now conform to basic seismic industry standards and can be read directly by popular seismic processing packages such as PROMAX. At present, only basic headers like FFID, Trace Number on File, and Receiver Channel Number, and Source Number are stored. From these basic headers, Trace Header Math can be used to recreate the source and receiver x-y coordinates. However, automatic inclusion of proper geometric headers in the trace headers at the time of acquisition is desirable. This will be done when we have reached a consensus as to what extra headers we should include and how we should define them.

With the SEG Y writing feature in place, even though only very basic header information is saved, we decided to conduct a trial experiment simulating a 3D marine seismic survey, in order to evaluate the performance of the modeling system for automatically collecting large datasets.

### **PHYSICAL DESCRIPTION OF THE TARGET**

Figure 1 is a photograph of the physical model used as the target. It consisted of a sheet of green silicone rubber molded to have two perpendicularly aligned anticlines on its upper surface. The bottom surface of the sheet is flat. The sheet is 600mm long by 470mm wide. In areas away from the anticlines, the thickness of the sheet increases linearly from 1mm at the left edge to about 3mm at the right edge. The thicknesses at the crests of the anticlines also vary; these thicknesses at different points on the anticline structure are listed in the caption of Figure 1.

The silicone rubber target was placed on top of an acrylic plate 600mm long by 470mm wide by 10mm thick. The two pieces were placed in a plastic container filled with de-mineralized water. We tried to keep the water level constant, but evaporation

over survey durations of up to 12 hours caused problems. The target and water-filled container were placed in the positioning coordinate system of the Modeling Facility with the long side of the target parallel to the X-axis.

## ACQUISITION

A linear array with 18 piezopin transducers separated by 10mm was constructed for the experiment to simulate a marine streamer. Applying the standard scaling factor of  $10^4$  to go from model units (mm) to world units (M), the transducer separation becomes 100m and the array length becomes 1700m (from this point on, all dimensions will be expressed in world units). The transducers at the ends of the array were used as transmitters (labeled TX-1 and TX-2), and the 16 transducers between them were used as receivers (labeled RX-1 to RX-16). The array was orientated along the Y-direction with TX-1 at (X=0, Y=0) and TX-2 at (X=0, Y=1700m).

Figure 2 is a photograph showing the array of piezopin transducers positioned over the target immersed in water. The view is looking towards negative X coordinates; Y coordinates increase towards the right.

Acquisition was done along lines in the Y-direction moving TX-1 from 0mm to 2500m in 50m steps, resulting in 51 inline source positions. For each source position, traces for the 16 receiver channels were recorded first with TX-1 active, and then with TX-2 active, giving 32 traces. Thus for each complete line in the Y-direction, 1632 traces were acquired. Once a line was completed, the array was moved back to Y=0, and then moved forward along the X-direction by 100m, so that second line begins with TX-1 coordinates of (X=100, Y=0). For the complete 3D survey, this procedure resulted in 33 lines for TX-1 positions that ranged from (X=0, Y=0) to (X=2700, Y=2500), with  $\Delta X=100\text{m}$  and  $\Delta Y=50\text{m}$ .

For this survey, over 50,000 traces were recorded over a total period of about 12 hours. Each trace consisted of 2000 digital points sampled every  $0.1\mu\text{s}$  with 14-bit precision. The dominant frequency in the source wavelet is about 1MHz. The scaling factor of  $10^4$  converts the sample interval and dominant frequency to world units of 1ms and 100Hz. The trace length in world units is 1999ms.

## RESULTS

The following plots show samples of raw data, with no processing other than sorting, bandpass filtering, and AGC.

### Common source gathers

The common source gathers (CSG) on Figure 3 display an example of data as they are acquired. Figure 3(a) shows the seismograms from the sixteen receivers when the first transmitter TX-1 is activated. Figure 3(b) shows the seismograms when the second transmitter TX-2 is activated. Figures 4(a) and 4(b) are two similarly acquired CSGs.

There is a dramatic difference between Figure 3 and Figure 4: the CSGs on Figure 3 have very strong events with linear moveout; on Figure 4, these are much weaker. On each gather, the early linear event is the direct arrival from transmitter to receiver, but the

later linear event is unexpected. That the two events are parallel leads us to speculate that the second event is an echo of the initial transmitted pulse along the length of the piezopin transmitter. The origin of the second linear event needs to be investigated further, and the event itself must be eliminated or attenuated before digitization in future work because it interferes with reflections.

The linear events on Figure 4 are much weaker because we took steps to deliberately decrease the amplitude of the direct arrival. This was done by either decreasing the length of the piezopin transmitting tip that is immersed in water, or by placing a small piece of attenuating foam around the transmitting tip. By decreasing the amplitude of the direct arrival and its echo on Figure 4, the reflections from the target at depth are much clearer than they are on Figure 3, since there is much less interference from the direct arrival and its echo.

### **Common offset gathers**

That reflections from targets at depth are improved when the direct arrivals are weak is emphatically indicated on Figure 5. Figure 5(a) shows a common offset gather with (transmitter-receiver offset equal to 100m), for the case where the direct arrivals are very strong. The reflection from the top of the anticline is barely discernible, and while the reflection (with pull-down) from the interface beneath the anticline is evident, the space-time coherence associated with it appears to be disrupted. In contrast, on the COG of Figure 5(b), the quality of the reflections from both the top and bottom of the anticline is excellent. The difference between Figures 5(a) and 5(b) is that on Figure 5(b), the much weaker direct arrival and its echo cause much less interference with the target reflections.

The pull-down of the reflection beneath the anticline can be used to estimate a velocity for the silicone rubber material. The pull-down at the crest of the anticline is about 320ms. The COG profile is in the Y-direction along a line to the left of the AB axis on Figure 1; at this position, the measured crest-to-bottom distance of the anticline is 160 m (16mm in model dimensions). The one-way pull-down time is 160ms, so we can estimate the velocity of the silicone rubber to be about 1000m/s.

Figure 6 is COG along the Y-direction, with the transmitter-receiver offset equal to 700m. The direct-arrival time is 470ms, as expected for the water velocity of 1480m/s. A reflection from the side of the plastic container is observed at the left side of the plot, beginning at about 1200ms and moving downwards in time towards the right with an apparent velocity of about 2980m/s. The reflection from anticline CD aligned in the X-direction is clearly visible, as is the reflection time pull-down beneath it due to the low-velocity silicone.

Figure 7 is a zoomed-in view of the anticline reflection on Figure 6. The two-way travel time to the crest of the anticline is observed to be about 1260ms. Taking into account the offset distance, this indicates that the depth to the crest of the anticline is about 860m.

Figure 8 shows a common offset gather along the X direction, with the transmitter-receiver offset equal to 500m. The zoomed-in view of the reflection from anticline AB

aligned parallel to the Y-axis clearly shows the convex-up shape of the anticline. Also visible is the pull-down of the reflection beneath the anticline. The two-way travel time to the crest of the anticline is observed to be about 1150ms. Accounting for the offset distance puts the depth to the crest of the anticline at about 813m.

### SUMMARY AND CONCLUSIONS

The test 3D marine survey conducted with the modernized Seismic Physical Modeling Facility produced encouraging results. The test survey indicated a number of improvements we need to make to our acquisition procedure. We summarize the main issues raised by the results of this experiment.

In our common source gathers, we observed very strong direct arrivals and multiples thereof. These multiples appear not to be reflection multiples, since their moveouts are parallel to the direct arrival moveouts. At present, we do not know their cause, but they are likely to be transmitter-related. We need to find out where they come from, and eliminate or attenuate them (before digitization, and not in processing) since they tend to disrupt the clarity and coherence of target reflections.

Reflections from the sides of the water-filled container are also a source of unwanted interference. They become less of a problem as the transducer array moves away from container boundaries, but steps to mute them before digitization should be investigated.

Our motivation in using piezopin transducers was that their small size made them convenient to using in arrays with multiple receivers and transmitters. In addition, their diameters of about 1mm scale up to only 10m in world units. Larger transducers with diameters of 5mm or 10mm scale up to unrealistic world footprints of 50 or 100m for receivers and sources. However, the problem with using the small piezopins is that their natural frequency response in water, whether transmitting or receiving, is about 1MHz (equivalent to a world frequency of 100Hz after scaling.). The corresponding wavelengths in water are about 1.48mm, making water-level control in the sub-millimeter range necessary. We have already commented on the dependence of the strength of direct arrivals on how deeply the piezopin transmitting tips are immersed. It is difficult to keep the water level constant during an entire survey if the survey duration exceeds 12 hours, as water evaporation slowly decreases it. One possible way of overcoming the evaporation problem may be to have a thin layer of non-volatile liquid such as hydraulic fluid floating on top of the water.

If we were to try to meet the Nyquist condition for spatial sampling with such small wavelengths, our grid sizes in the X-Y plane must be less than 1mm. This increases both survey time and dataset volume to the point where a realistic 3D survey becomes impractical. The short wavelengths and likely spatial aliasing may also cause problems for processing. We may need to compromise on the conflicting desires for small footprints and for longer wavelengths, and consider using larger transducers (say, with diameters of 5mm) with lower natural frequencies in the range 0.3 to 0.5Mz.

Future work for this model will include conducting a second 3D survey with line orientations at 45 degrees to the axes of the anticlines. The combined datasets will undergo 3D processing to produce 3D images of the target.

Our approach for 3D marine acquisition of using multiple 2D lines gives us narrow-azimuth (NAZ) coverage, and is considered primitive as far as modern industry practice is concerned. As we continue to modify and upgrade our acquisition hardware, software, and procedures, we will undertake more elaborate marine surveys using wide-azimuth (WAZ) and rich azimuth (RAZ) designs (Sukup, 2002; Howard, 2007). These surveys will involve separate multi-transmitter and multi-receiver arrays orientated at right angles so that multi-azimuth (MAZ) acquisition and true 3D binning are enabled.

### **ACKNOWLEDGEMENTS**

We thank the industrial sponsors of CREWES and NSERC for supporting this research. We are grateful to Landmark Geophysical Inc. for providing access to the PROMAX seismic processing package.

### **REFERENCES**

- Howard, M., 2007. Marine seismic surveys with enhanced azimuth coverage: lessons in survey design and acquisition, *The Leading Edge*, **26**, 480-493.
- Sukup, D.V., 2002. Wide azimuth marine acquisition by the helix method: *The Leading Edge*, **21**, 791-794.
- Wong, J., Hall, K.W., Gallant, E.V., Maier, R., Bertram, M.B., and Lawton, D.C., 2009. Seismic physical modeling at the University of Calgary: *CSEG Recorder*, **34**, 36-43.

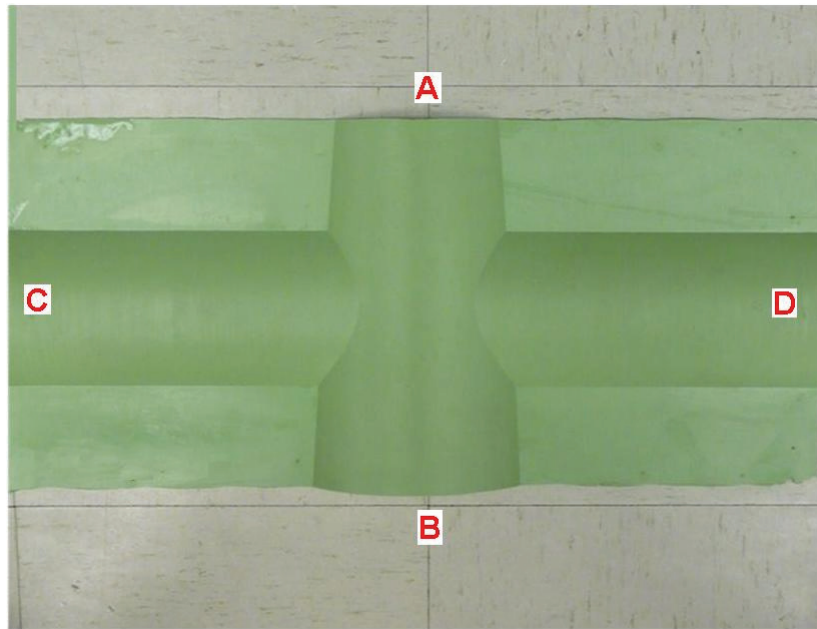


FIG 1: Photograph of the silicone rubber target with crossed anticlines on the reflecting surface. The widths  $W$  and thicknesses  $T$  of the anticlines vary. At Point A,  $W=116\text{mm}$ ,  $T=17\text{mm}$ ; at point B;  $W=153\text{mm}$ ,  $T=32\text{mm}$ ; at point C,  $W=113$ ,  $T=16\text{mm}$ ; at point D,  $W=113\text{mm}$ ,  $T=18\text{mm}$ . In the areas not occupied by the anticlines, the thickness varies slightly between 1mm and 3mm. The bottom surface of the target is flat. Positive X-direction is C to D; positive Y-direction is B to A.

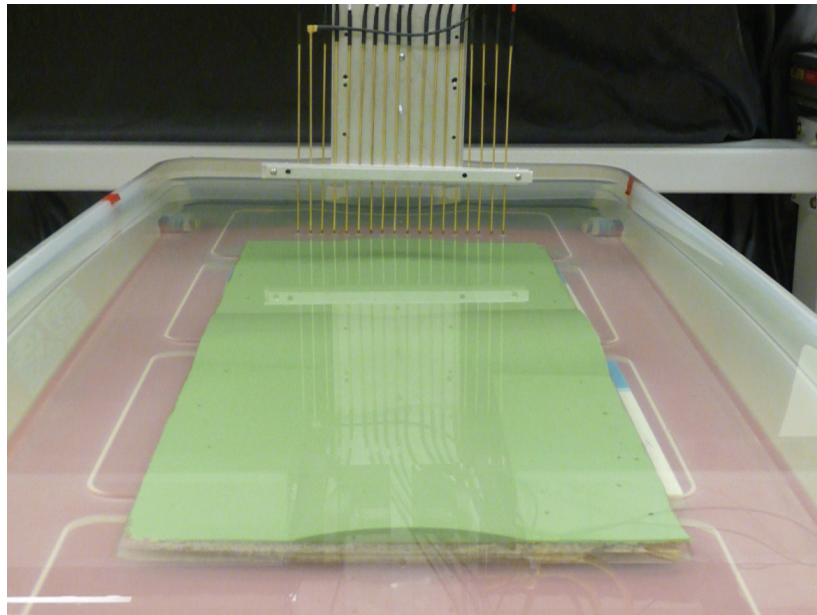


FIG 2: An array of 16 receiving piezopin transducers between 2 transmitting transducers, positioned over the molded silicone rubber target immersed in water.

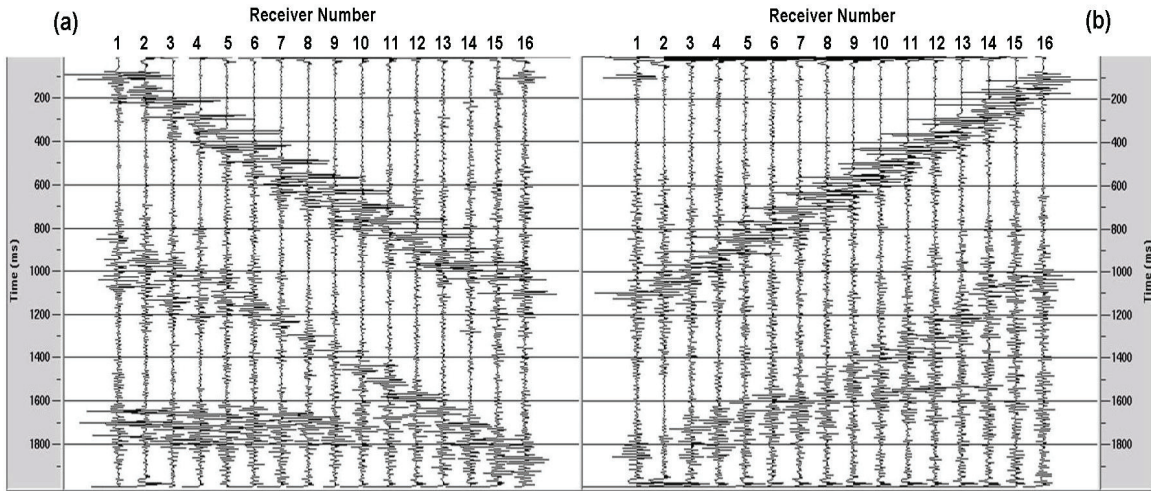


FIG. 3: Common source gathers showing the strong direct arrival and its echo that interfere with deep reflections.

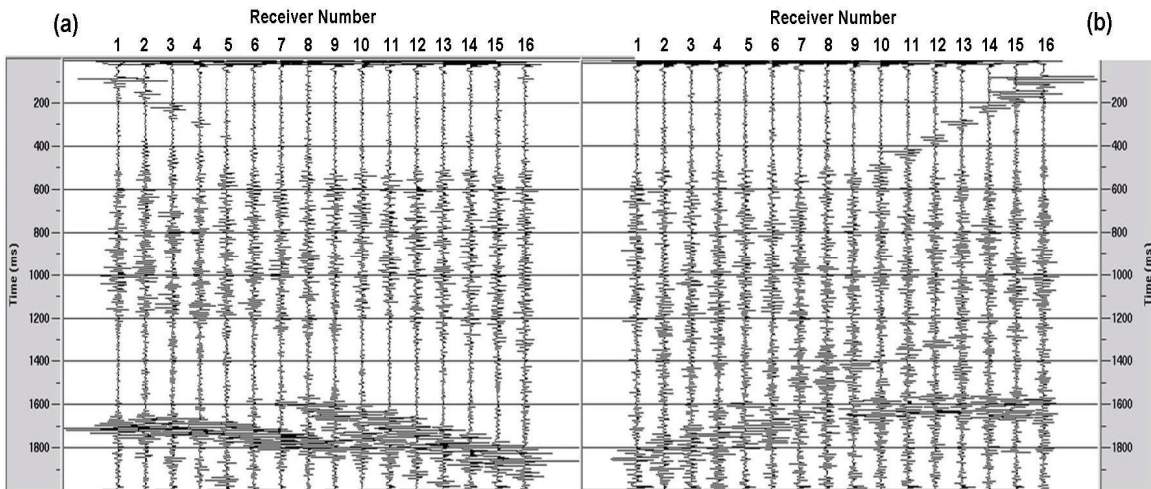


FIG. 4: Common source gathers showing much the much weaker direct arrival and no echo; there is minimal interference with deep reflection events of interest.

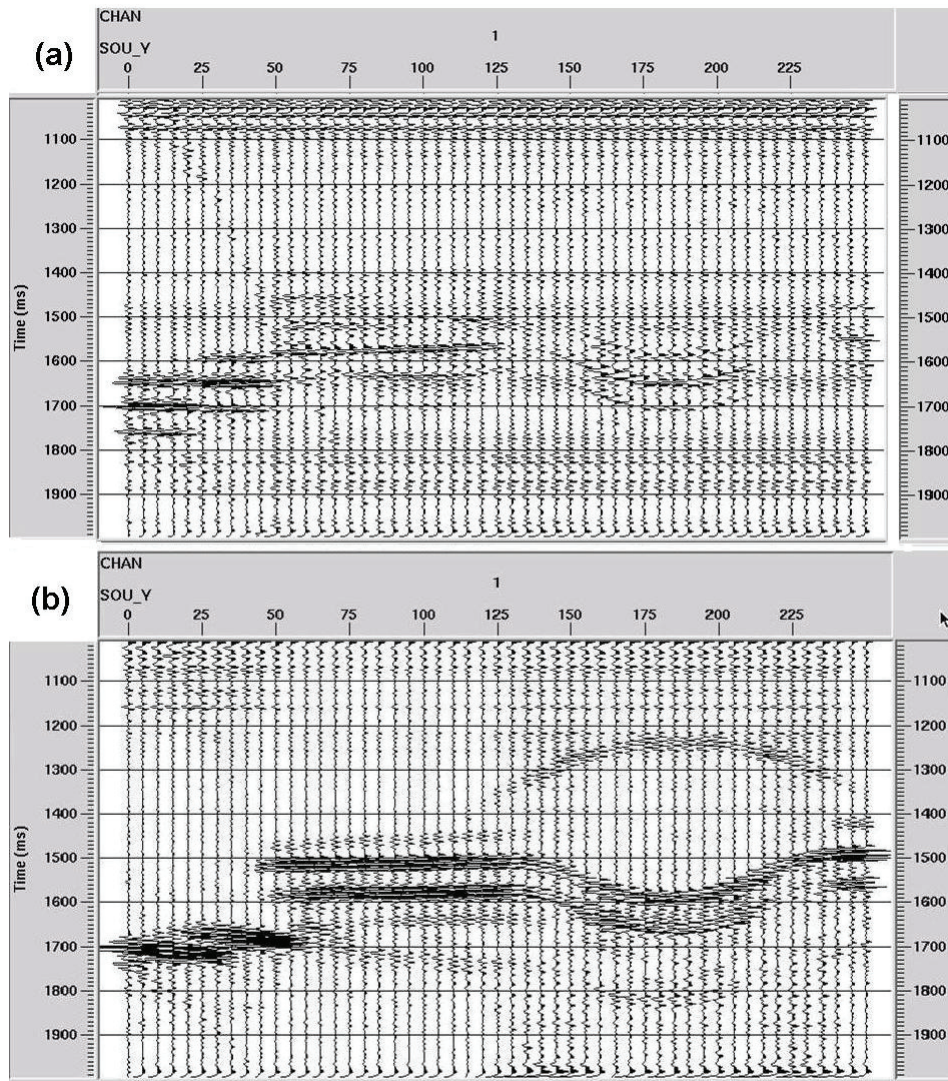


FIG. 5: Common offset gather (offset=100m) showing the improvement in quality of deep reflections when the strong direct arrival and its echo are absent. (a) COG for seismograms from the seismogram set as in Figure 3, where the direct arrival and its echo are very strong. (b) COG for seismograms from the seismogram set as in Figure 4, where the direct arrival and its echo are much weaker.

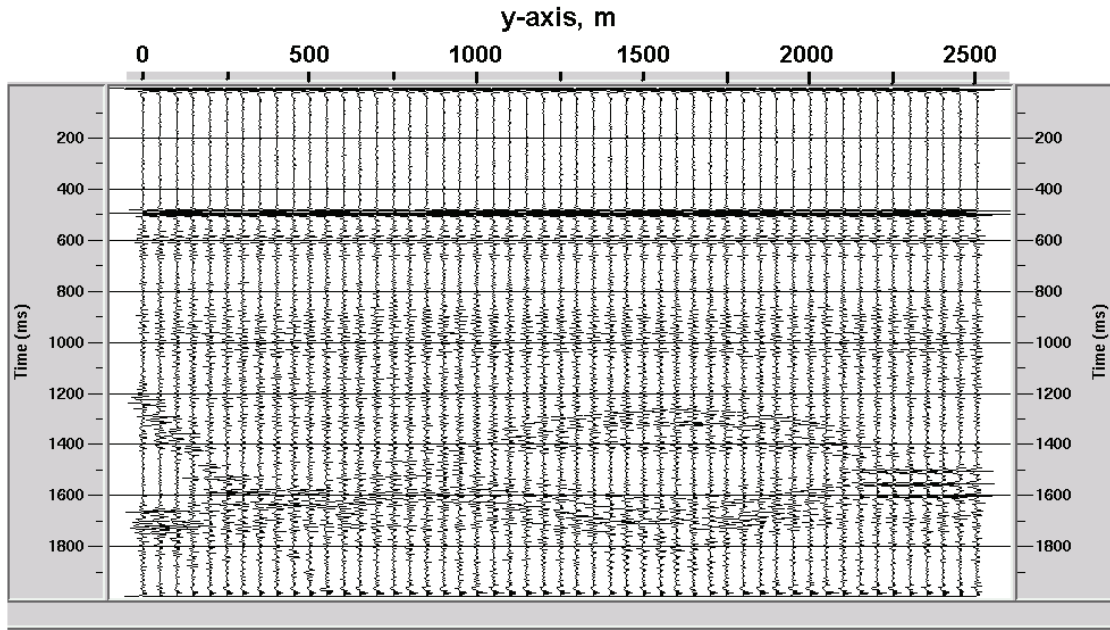


FIG. 6: A common offset gather (offset=700m) along the Y-direction. The direct arrival is the horizontal event at 473ms. A side reflection occurs on the left-hand-side beginning at a time of 1200ms. The reflection from the anticline is clearly visible. Note the pull-down beneath the low-velocity silicone anticline.

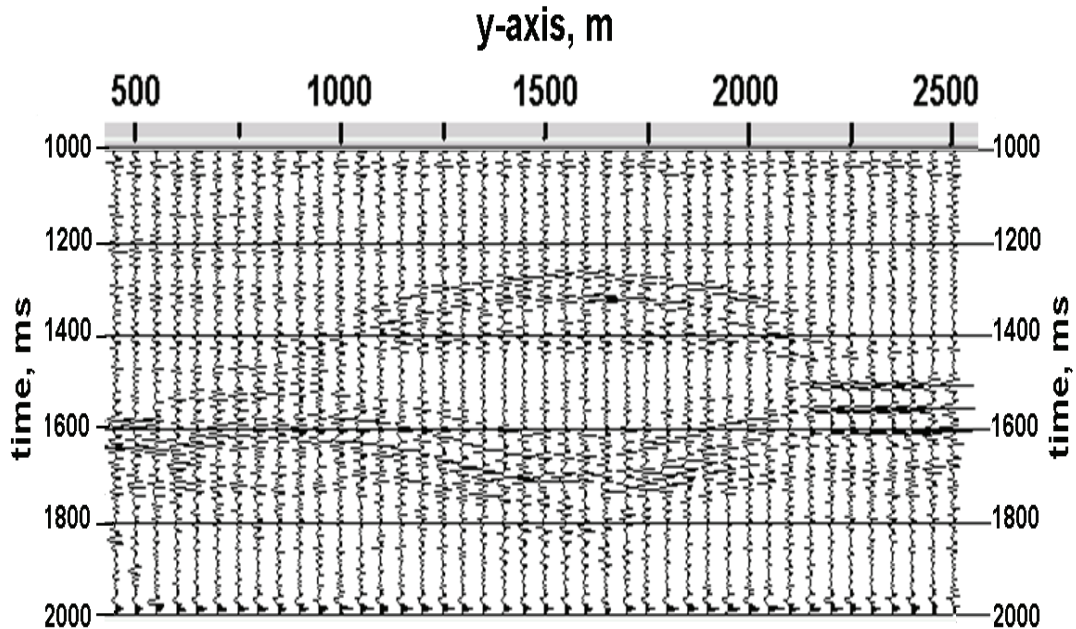


FIG. 7: Expanded view of the COG on Figure 6, emphasizing the reflection from the anticline. The two-way time at the crest of the anticline is about 1260ms.

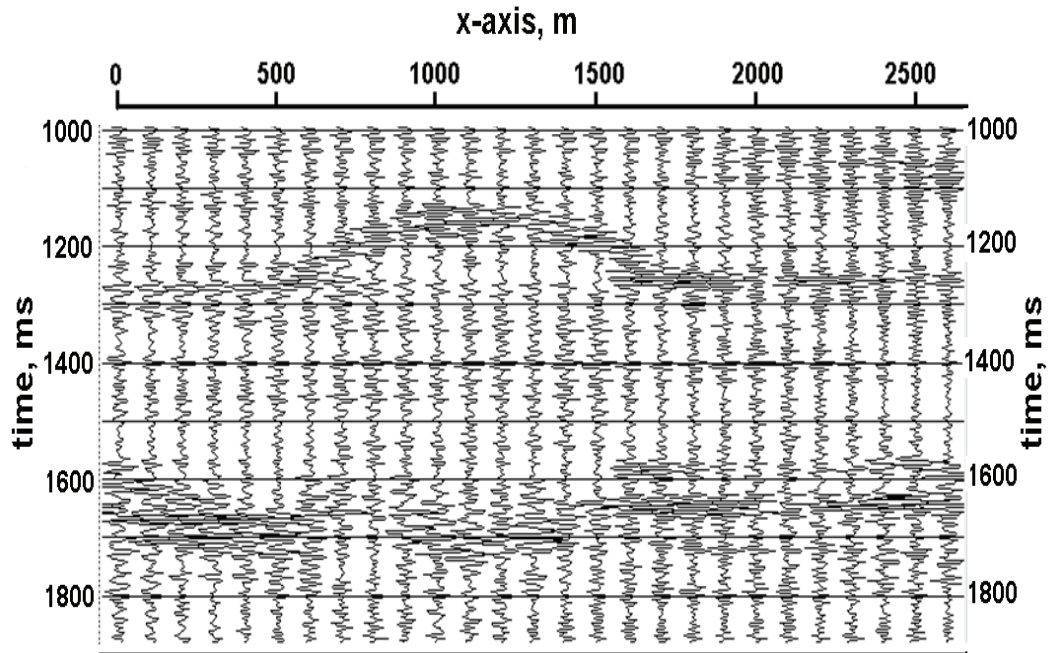


FIG. 8: A common offset gather (offset=500m) along the x-direction. The reflection from the top of the anticline and the pull-down due to the low-velocity silicone are clearly visible.